J. Phys. B: At. Mol. Opt. Phys. **31** (1998) 2601–2609. Printed in the UK PII: S0953-4075(98)88277-1

Electron bremsstrahlung in collisions of 223 MeV/u He-like uranium ions with gaseous targets

T Ludziejewski†††, Th Stöhlker‡†, S Keller§, H Beyer†, F Bosch†, O Brinzanescu†, R W Dunford‖, B Franzke†, C Kozhuharov†, D Liesen†, A E Livingston¶, G Menzel†, J Meier†, P H Mokler†, H Reich†, P Rymuza[+], Z Stachura[*], M Steck†, L Stenner†, P Świat[#] and A Warczak[#]

† Gesellschaft für Schwerionenforschung, D-64220 Darmstadt, Germany
‡ University of Frankfurt, D-60486 Frankfurt, Germany
§ University of Frankfurt, D-60054 Frankfurt, Germany
‖ Argonne National Laboratory, Argonne, IL 60439 USA
¶ University of Notre Dame, Indiana 4556, USA
[+] Institute for Nuclear Studies, 05-400 Świerk, Poland
[*] Institute of Nuclear Physics, 31-342 Cracow, Poland
[#] Jagiellonian University, 30-059 Cracow, Poland

Received 8 October 1997

Abstract. The bremsstrahlung process in the domain of strong Coulomb fields has been investigated for N_2 and Ar target electrons colliding with He-like uranium ions at 223 MeV/u. The differential cross sections for bremsstrahlung were measured at laboratory observation angles of 48°, 90°, and 132°. Substantial discrepancies were found between the experimental cross sections and the first-order Born approximation calculations. The reported data provide a new testing ground for non-perturbative treatment of the coupling between radiation and matter in the presence of strong fields.

1. Introduction

Intensive experimental and theoretical efforts have been devoted to the study of electron–atom bremsstrahlung over a wide range of electron energies up to the GeV regime (for a review see e.g. Koch and Motz 1959, Pratt and Feng 1985 and references therein). These studies have established that the relativistic Born approximation (Bethe and Heitler 1934), modified by screening and Coulomb corrections is capable of describing fairly well the experimental data for moderate values of the characteristic parameter $Z\alpha/\beta$, where Z is the target nuclear charge, α is the fine structure constant, and β is the electron velocity in units of the speed of light. For the case of high-Z targets computationally much more sophisticated approximations (Elwert and Haug 1969) and exact all-order calculation schemes (Tseng and Pratt 1971, Tseng *et al* 1977) have been developed.

Bremsstrahlung is also an important x-ray production mechanism in ion–atom collisions. Here, the predominant source of bremsstrahlung is inelastic scattering of initially bound target electrons by the nucleus of the projectile. For not too heavy targets, the cross section for this process is given by the bremsstrahlung cross sections for electrons moving with

†† Permanent address: Sołtan Institute for Nuclear Studies, 05-400 Otwock-Świerk, Poland. E-mail address: T.Ludziejewski@gsi.de

0953-4075/98/112601+09$19.50

projectile speed multiplied by the number of available target electrons. The underlying assumption is that this process can be treated within the framework of the impulse approximation, i.e. the loosely bound electrons can be treated as quasifree particles.

In the last two decades electron bremsstrahlung accompanying ion–atom collisions has been thoroughly investigated for intermediate projectile energies (Jakubaßa and Kleber 1975, Ishii *et al* 1977, Yamadera *et al* 1981, Ishii and Morita 1985, Ozawa *et al* 1986, Ishii *et al* 1993, Tawara *et al* 1997). In this energy domain the adaptation of the relativistic Born approximation together with the impulse approximation generally gives reasonable agreement with the experimental data.

The major advantage of ion–atom collisions for the study of bremsstrahlung is that the charge state of the projectile can be easily and selectively varied. The case of bare ions attracts the greatest interest since here the interaction of the electrons with the pure Coulomb potential of the projectile can be studied in the absence of many-body effects. Hence, the reliability of theoretical models can be most rigorously examined in such experiments. In particular, high-Z projectiles are of interest, as they exclusively probe the coupling between the continuum states and the radiation field in the presence of strong external potentials. To the best of our knowledge, only one study of this type has been reported in the literature (Anholt *et al* 1986). In that experiment differences up to a factor of 3 were observed between the experimental results and the predictions of the Coulomb corrected Bethe–Heitler formula. This study also established that solid targets pose problems which arise from secondary electron bremsstrahlung, in particular when dealing with forward observation angles. Precise knowledge of bremsstrahlung cross sections is also important from a practical point of view since bremsstrahlung constitutes a serious source of background radiation in all ion–atom collision experiments (Folkmann *et al* 1974a, b, Sohval *et al* 1975).

This paper reports measurements of the differential cross sections for bremsstrahlung produced by 223.2 MeV/u He-like uranium impinging upon N_2 and Ar gaseous targets. Particular attention has been paid to the tip region (hard photon emission) of the spectrum since this energy domain is, in particular, sensitive to Coulomb distortions caused by the large nuclear charge of the projectile. Moreover, it is well established (Fano 1959, McVoy and Fano 1959, Andersson and Burgdörfer 1993) that hard-photon bremsstrahlung is closely related to the radiative recombination, i.e. the time-reversed photo-electric effect. The bremsstrahlung process may be interpreted as radiative recombination (RR), or radiative electron capture (REC) to positive energy states of the projectile, and indeed the matrix elements for the tip-region can be obtained by analytic continuation of those for REC. The latter process has been intensively studied theoretically as well as experimentally even for the highest nuclear charges (Ichichara *et al* 1994, Eichler *et al* 1995, Stöhlker *et al* 1995, 1997). This investigation is complementary to these studies in that it extends them to final electron states of positive energy.

2. Experimental arrangement

The measurements were performed at the SIS-ESR (heavy ion synchrotron—experimental storage ring) facility at the Gesellschaft für Schwerionenforschung (GSI) in Darmstadt. U^{73+} ions were delivered by the SIS synchrotron and after passing a stripper, the magnetically separated fraction of U^{90+} ions was injected into the ESR storage ring. Up to the 10^8 uranium ions were accumulated in the ESR ring after completion of the stacking procedure. The beam was continuously cooled by the electron-cooler device providing excellent beam quality with a typical momentum spread $\Delta p/p \leqslant 10^{-4}$ and the corresponding transverse emittance of the order of 0.1π mm mrad^{-1} with beam diameters of about 5 mm. The final

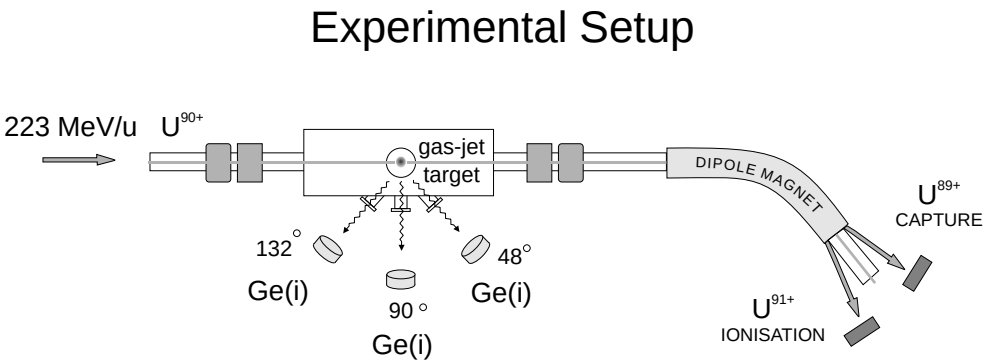

Figure 1. Schematic view of the experimental arrangement at the internal gas-jet target of the ESR storage ring.

beam energy, defined by the electron-cooler voltage, was equal to 223.2 MeV/u. After completion of the stacking procedure, the internal gas-jet target was switched on. Argon and molecular nitrogen gaseous targets with areal densities between 10^{11} and 10^{12} particles/cm^2 were used.

The experimental arrangement at the internal gas-jet target of the ESR storage ring is schematically illustrated in figure 1. The x-ray emission from the target area was measured by three Ge(i) detectors placed at 48°, 90°, 132° with respect to the beam axis. In order to reduce the Doppler broadening the detectors at 48° and 90° were equipped with collimators consisting of copper and lead layers forming 5 mm wide slits. The 48° and 132° detectors were separated from the high vacuum by 100 μm Be windows, while a 50 μm stainless steel window was used at 90°. As depicted in the figure, downstream from the gas-jet area two particle detectors (NE110 plastic scintillators) were used in order to register uranium ions which captured or lost one electron. These detectors, located behind the first dipole magnet downstream from the gas-jet target area registered electron capture or projectile ionization events with an efficiency very close to 100%. Details of the experimental arrangement at the gas-jet target of the ESR storage ring as well as a description of the data acquisition system can be found in Stöhlker *et al* (1995).

3. Data analysis and results

In figure 2 x-ray spectra measured at 132° for U^{90+} on N_2 are shown. The upper plot shows a single spectrum, i.e. it was accumulated without any coincidence condition. The x-ray continuum seen in the spectrum is due to primary and secondary electron bremsstrahlung. For x-ray energies below the indicated endpoint, this continuum is essentially caused by the primary bremsstrahlung. The endpoint energy is given by $E_{\max} = (\gamma - 1)mc^2\gamma^{-1}(1 - \beta\cos\Theta)^{-1} = 70.8$ keV, where β is the projectile velocity in units of the speed of light, $\gamma = (1 - \beta^2)^{1/2}$, mc^2 is the electron rest mass in keV, and Θ is the observation angle in the laboratory frame. Above this endpoint, the x-ray continuum is mainly due to secondary electron bremsstrahlung (SEB). The SEB originates from the target electrons ejected in the primary collision and then rescattered in the target material with the emission of bremsstrahlung. For this process the endpoint energy is given in the classical limit by $4 \times E_{\max}$. The SEB seems to be unimportant for gas targets with areal densities of about 10^{12} particles/cm^2. Indeed, Sohval *et al*

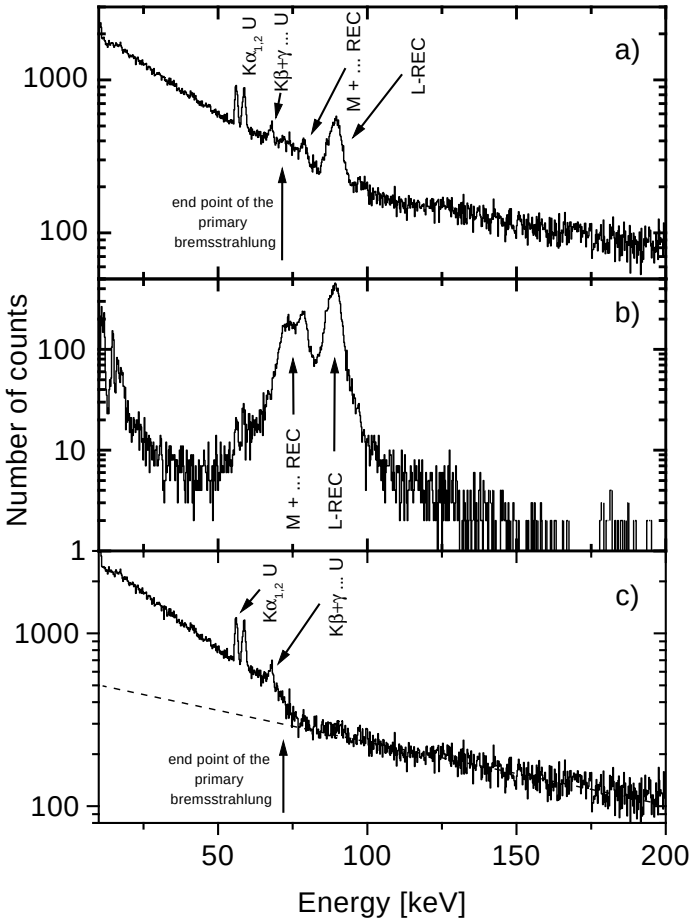

Figure 2. X-ray spectra for 223.2 MeV/u U^{90+} on N_2 collisions recorded (*a*) without, and (*b*) in coincidence with down-charged U^{89+} ions. The positions of the characteristic radiation of projectile, of the endpoint of the primary bremsstrahlung, as well as positions of REC leading to the L, M and higher shells are marked by arrows. The data shown in (*c*) represent the spectrum corrected for x-rays associated with electron capture and corrected for the efficiency of the x-ray detectors. The broken curve shows the result of the least squares fit of the background radiation.

(1975) estimated that for intermediate energy ion–atom collisions the cross section for SEB becomes comparable with the primary bremsstrahlung or REC cross sections for targets densities above 10^{18} particles per cm^2. In our case, however, the emission of SEB may occur in the walls of the scattering chamber or detector windows as well.

Apart from bremsstrahlung, the discrete lines of the characteristic projectile radiation can be seen together with REC into the L- and M- and higher shells. The $K\alpha$ and $K\beta$ radiation is produced here by the Coulomb excitation of the K-shell electrons. The spectrum shown in figure 2(*b*) was taken in coincidence with down-charged U^{89+} ions. As seen in the figure, the coincident spectrum is dominated by L- and M-REC radiation (K-REC as well as characteristic K x-rays of the projectile are not present due to the occupied K-shell of the projectile). A comparison of figure 2(*a*) with figure 2(*b*) demonstrates that in order

to determine the shape of the bremsstrahlung spectrum near its endpoint it is essential to measure the contribution of the x-ray radiation associated with electron capture processes.

In order to evaluate the primary bremsstrahlung spectrum the following procedure was applied. The spectra were calibrated for energy and efficiency. In addition, the spectra taken at 90° were corrected for absorption of low-energy photons in the stainless steel window using tabulated photo-absorption cross sections of Storm and Israel (1970). The coincidence acquisition mode allowed us to disentangle the bremsstrahlung spectra from the L-REC and M-REC radiation which would mask the details of the bremsstrahlung spectrum near its endpoint. This was accomplished by subtracting the coincidence spectrum from the corresponding singles spectrum. The resulting spectrum is plotted in figure 2(c). Finally, the spectra for primary bremsstrahlung were corrected for background radiation (SEB as well as possible high energy photons due to Compton scattered γ-rays). This background was estimated by using a least-square fit to the continuum radiation seen above the endpoint for primary bremsstrahlung assuming a power-law behaviour (Jakubaßa and Kleber 1975, Sohval *et al* 1975). In order to put the obtained relative cross section data on the absolute scale, the spectra were normalized to theoretical L-REC cross sections for 132°. The latter were obtained from all-order relativistic calculations according to Ichihara *et al* (1994) and Eichler *et al* (1995). These calculations are known to describe very well the available experimental data for REC into high-Z projectiles (Stöhlker *et al* 1995). In particular, it has been demonstrated by Stöhlker *et al* (1994) that this model yields good quantitative agreement with experimental subshell resolved angular distributions of L-REC for He-like uranium. We expect that for the observation angles of relevance the uncertainty of the theoretical prediction (due to the use of hydrogen-like wave-functions for the electron in the final state) does not exceed a few per cent. In order to extract information about the total number of radiative electron capture events, the L-REC lines observed at 13° were fitted by means of a least square method taking into account the Compton profile of the target electrons as well as additional Doppler broadening caused by the finite angular acceptance of the x-ray detectors. The momentum distribution of the target electrons were taken from Hartree–Fock calculations of Biggs *et al* (1975). We estimate that the overall uncertainty of the differential cross sections stemming from the applied spectrum analysis and normalization procedure does not exceed 20%.

As an additional check of our results the x-ray yield measured by the individual detectors were normalized to the charge exchange rate measured by the particle detector for electron loss and by using theoretical electron loss cross sections taken from Trautmann and Rösel (1980). This theory is known to give reliable cross section predictions with a precision of about 30% (Rymuza *et al* 1993). Within this uncertainty the result of the latter method agrees well with the former normalization procedure.

4. Discussion

In figure 3 the experimental cross sections for bremsstrahlung production in collisions of U^{90+} with N_2 and Ar are compared with the predictions of the relativistic Born approximation. The theoretical curves shown have been obtained by adapting the Bethe–Heitler formula as quoted by Koch and Motz (1959). Since standard bremsstrahlung theory is formulated in the rest frame of the scattering centre, a Lorentz transformation to the laboratory frame (see e.g. Eichler and Meyerhof 1995) had to be introduced (note that a projectile kinetic energy of 223.2 MeV/u corresponds to Lorentz parameter β of 0.591, or to 122.44 keV of an electron kinetic energy in the projectile rest frame). The calculated cross sections were corrected for Doppler broadening and convoluted with the momentum

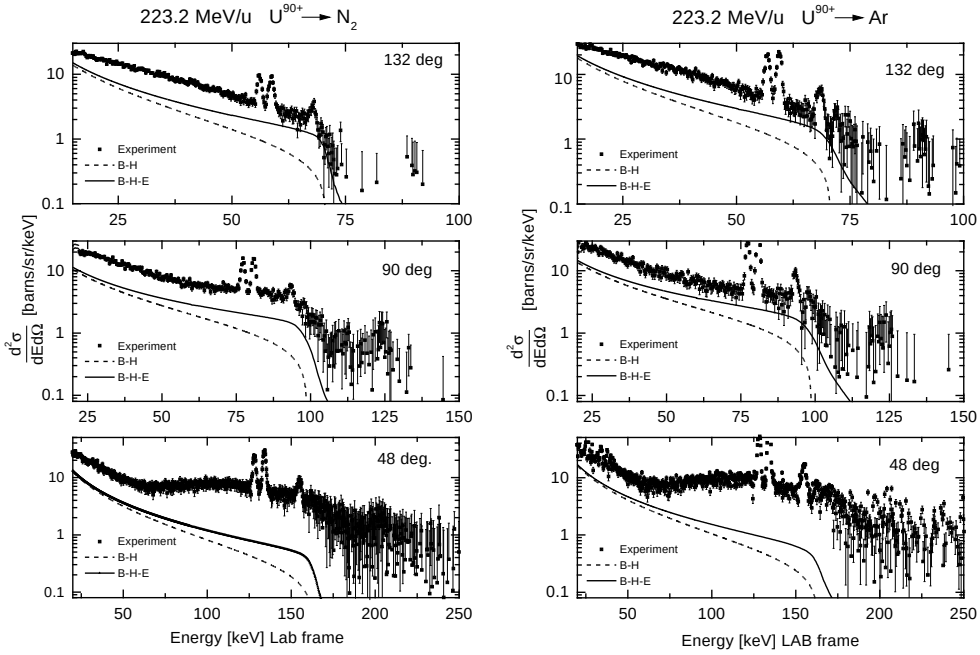

Figure 3. Doubly differential cross sections for bremsstrahlung emission in collisions of 223.2 MeV/u U^{90+} with N_2 (left) and Ar (right) for laboratory observation angles $\Theta = 132^\circ$, $\Theta = 90^\circ$, and $\Theta = 48^\circ$. The experimental data are compared with the predictions of Bethe–Heitler–Elwert calculations taking into account the Compton profile of target electrons and the Doppler broadening (B–H–E—full curve). For reference, results of Bethe–Heitler formula are shown (B–H—broken curve). The error bars of the experimental data represent only the uncertainty due to counting statistics.

distribution of the initial electron bound states. Indeed, just like the REC line profile, the shape of the bremsstrahlung spectrum near its endpoint reflects the momentum distribution of the target electrons.

The Bethe–Heitler formula fails to predict a non-zero doubly differential cross sections at the tip of the photon spectrum. This is a consequence of the fact that high-energy photons arise from collisions where the final electron velocity is close to zero ($\beta \simeq 0$). Here, the condition of validity of the first Born approximation $Z\alpha/\beta \ll 1$ is not satisfied. In a first approximation this defect can be eliminated by multiplying the results obtained from the Bethe–Heitler formula with the so-called Elwert correction (Elwert 1939). This approach (Bethe–Heitler–Elwert model) takes into account in an approximate way the fact that the low-energy electron wavefunctions in the final state are perturbed by the Coulomb field of the nucleus by considering the non-relativistic Coulomb densities of the initial and final electron states. It has been demonstrated (see e.g. Pratt and Tseng 1975) that this correction generally leads to an improved agreement between experiment and theory even in the domain of relativistic energies and high-Z systems.

Figure 3 compares measured with calculated cross sections for U^{90+} impact on N_2 and Ar targets. In order to demonstrate the influence of the Elwert correction and Compton plus Doppler broadening of the endpoint energy region the predictions of the Bethe–Heitler formula are shown in addition. At 132° and 90° the shape of the experimental spectrum is reasonably well described by the Bethe–Heitler–Elwert calculations, however the absolute

magnitude of the cross sections is underestimated by approximately a factor of 2. A similar trend is observed for the low-energy regime at 48°, while at large photon energies, an additional continuum shows up in the x-ray spectrum. This rise of the cross section is in contrast to standard theories (which predict gradually decreasing photon yields as a function of the energy) and therefore cannot be explained in terms of primary electron bremsstrahlung.

For He-like high-Z systems one has to consider an additional source of x-ray continuum emission. The $K\alpha_1$ and $K\alpha_2$ radiation which can be seen in figures 2 and 3 originates from the Coulomb excitation of the ground-state electrons to the P states of the projectile. However this mode of excitation similarly populates $2\,^1S_0$ state which then decays solely by the two photon (2E1) emission. This radiation manifests itself as a broad symmetric structure extending from zero energy to approximately energy of the $K\alpha_2$ radiation. This excitation mode is likely to be responsible for a small enhancement of x-ray yields at moderate photon energies. However, in view of its strength, the additional continuum observed at 48° cannot be attributed to the two-photon decay of $2\,^1S_0$ state populated by the Coulomb excitation. Furthermore, according to the calculations of Jakubaßa and Kleber (1975), the high values observed for the doubly differential cross sections also cannot be explained by the nuclear bremsstrahlung or radiative ionization of the projectile electrons. Since the solid-state detectors used do not allow us to distinguish between photon and electron impact, we are inclined to presume that this feature should be ascribed to electrons emitted in forward direction. It is possible that these electrons could either be directly registered in our detector or could produce radiation in the detector windows or adjacent walls of the scattering chamber.

It is evident from figure 3 that the Bethe–Heitler–Elwert model cannot predict the correct absolute magnitude of bremsstrahlung cross sections. This result indicates a breakdown of the Born approximation in the domain of investigated impact energy and projectile atomic number. In order to check our interpretation, we have converted the tabulated results of the all-order benchmark calculations for electron–neutral uranium scattering at 100 keV impact published by Kissel *et al* (1983) to inverse collision kinematics, and compared this with the Bethe–Heitler–Elwert model. We find that indeed the substantial discrepancies (up to a factor of 2) between first- and all-order data are present for the domain of angles investigated.

Figure 4 shows the angular distribution of the bremsstrahlung spectra for energies equal to 25, 50, 65 keV for the N_2 and the Ar target, respectively. The energies were chosen to avoid overlap with the characteristic radiation of the projectile and the enhanced radiation intensity observed at 48°. The plot confirms the observed discrepancies between the experimental data and the Bethe–Heitler–Elwert model. It is worth noting that both the experimental and theoretical cross sections plotted in figure 4 vary slowly as a function of the observation angle in the laboratory frame. This points to an approximate cancellation between retardation and Lorentz transformation, an effect well known from studies of REC (see e.g. Spindler *et al* 1979, Stöhlker *et al* 1997).

5. Summary and conclusions

We have measured the differential cross sections for bremsstrahlung accompanying collisions of 223.2 MeV/u U^{90+} with gaseous N_2 and Ar targets at various observation angles. The measurements were performed at the ESR storage ring. The brilliant heavy-ion beams of the ESR along with the low-density gas targets allowed us to minimize significantly the influence of various unwanted processes such as the radiation associated with REC into the L, M and higher projectile shells and secondary electron bremsstrahlung.

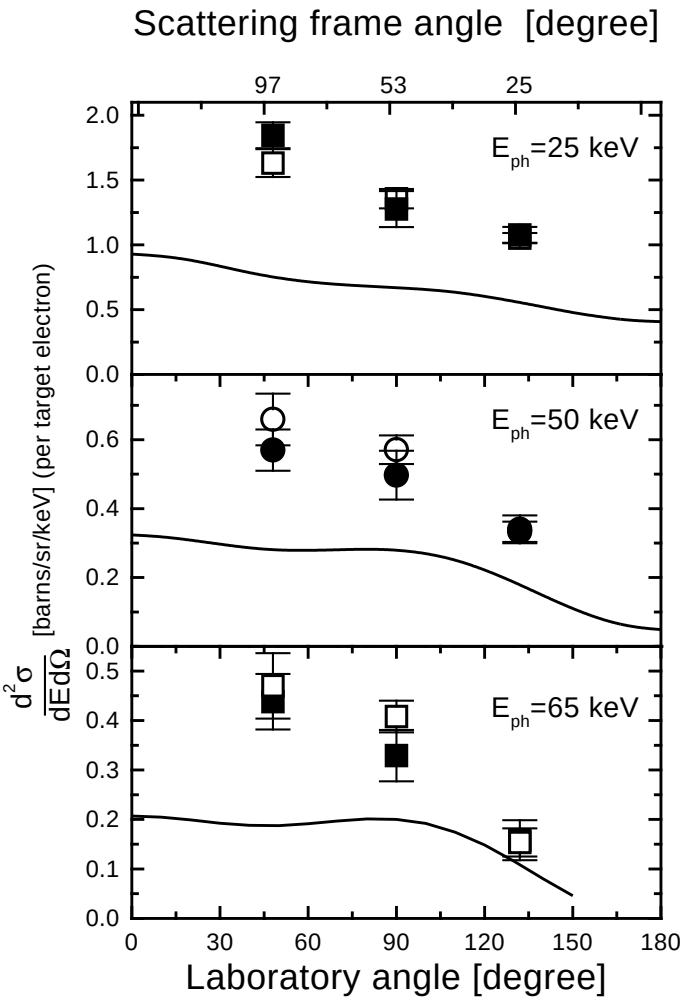

Figure 4. Angular distribution of target electron bremsstrahlung in collisions of 223.2 MeV/u U^{90+} with gaseous N_2 (open symbols) and Ar (full symbols) targets. Doubly differential cross sections at 25, 50, and 65 keV are given per target electron. The solid lines represent Bethe–Heitler–Elwert calculations of the primary bremsstrahlung. The corresponding photon emission angle in the scattering frame (180°—projectile frame angle) is given on the upper axis.

The results reported offer a new testing ground for 'complete' theories, and theoretical models going beyond the first terms of a $Z\alpha$ expansion series. Indeed the comparison of our data with the first-order Bethe–Heitler–Elwert formula shows the necessity of the use of higher- or all-order calculations (taking into account the ionic boundary conditions) to describe quantitatively the production of bremsstrahlung in relativistic collisions with highly charged heavy ions. Moreover, these data can be used to estimate the background radiation which is a limiting factor, for example in 1s Lamb-shift experiments based on calorimetric techniques (Egelhof 1996).

We expect that future studies of bremsstrahlung continua in such collisions will, in particular, allow us to investigate the interrelations between bremsstrahlung and REC in the non-perturbative regime. For this purpose a dedicated experimental set-up will

be implemented at the gas target reaction chamber of the ESR. Here, complete angular distribution measurements would be feasible while possible background caused by secondary electron production can be efficiently eliminated.

Acknowledgments

We would like to acknowledge the helpful discussion with D A Jenkins. Partial support for this work was provided by the Polish Committee for Scientific Research (KBN) grants no 2 P 302 119 07 and no 2 P 03 B10 910. RWD was supported by GSI and the US DOE office of basic energy sciences.

References

Andersson L R and Burgdörfer J 1993 *The Physics of Electronic and Atomic Collisions (AIP Conf. Proc. 295)* (New York: AIP) p 595
Anholt R *et al* 1986 *Phys. Rev.* A **33** 2270
Bethe A H and Heitler W 1934 *Proc. R. Soc.* A **146** 83
Biggs F, Mendelsohn L B and Mann J B 1975 *At. Data Nucl. Data Tables* **16** 201
Egelhof P, Beyer H F, McCammon D, Feilitzsch F, Kienlin A, Kluge H-J, Liesen D, Meier J and Stöhlker 1996 *Nucl. Instrum. Methods Phys. Res.* A **370** 263
Eichler J, Ichihara A and Shirai T 1995 *Phys. Rev.* A **51** 3027
Eichler J and Meyerhof W E 1995 *Relativistic Atomic Collisions* (San Diego: Academic)
Elwert G 1939 *Ann. Phys., Lpz.* **34** 178
Elwert G and Haug E 1969 *Phys. Rev.* **183** 90
Fano U 1959 *Phys. Rev.* **116** 1156
Folkmann F, Borggreen J and Kjeldgaard A 1974a *Nucl. Instrum. Methods* **119** 117
Folkmann F, Gaarde C, Huus, T and Kemp K 1974b *Nucl. Instrum. Methods* **116** 487
Ichihara A, Shirai T and Eichler J 1994 *Phys. Rev.* A **49** 1875
Ishii K, Kamiya M, Sera K, Morita S and Tawara H 1977 *Phys. Rev.* A **15** 2126
Ishii K, Maeda K, Takami M, Sasa Y, Uda M and Morita S 1993 *Nucl. Instrum. Methods Phys. Res.* A **75** 73
Ishii K and Morita S 1985 *Phys. Rev.* A **31** 1168
Jakubaßa D H and Kelber M 1975 *Z. Phys.* A **273** 29
Kissel L, Quarles C A and Pratt R H 1983 *At. Data Nucl. Data Tables* **28** 381
Koch H W and Motz J W 1959 *Rev. Mod. Phys.* **31** 920
McVoy K W and Fano U 1959 *Phys. Rev.* **116** 1168
Nakel W 1994 *Phys. Rep.* **243** 317
Ozawa K, Chang J H, Yamamoto Y, Morita S and Ishii K 1986 *Phys. Rev.* A **33** 3018
Pratt R H and Feng I J 1985 *Atomic Inner Shell Processes* ed B Crasemann (New York: Plenum)
Pratt R H and Tseng H K 1975 *Phys. Rev.* A **11** 1797
Rymuza P *et al* 1993 *J. Phys. B: At. Mol. Opt. Phys.* **26** L169
Sohval A R, Delavaille J P, Kalata K and Schnopper H W 1975 *J. Phys. B: At. Mol. Phys.* **8** L426
Spindler E, Betz H-D and Bell F 1979 *Phys. Rev. Lett.* **42** 832
Stöhlker Th *et al* 1994 *Phys. Rev. Lett.* **73** 3520
Stöhlker Th *et al* 1995 *Phys. Rev.* A **51** 2098
Stöhlker Th, Mokler P H, Kozhuharov C and Warczak A 1997 *Comment. At. Mol. Phys.* **33** 271
Storm E and Israel H I 1970 *Nucl. Data Tables* A **7** 565
Tawara H, Azuma T, Ito T, Komaki K, Yamazaki Y, Matsuo T, Tonuma T, Shima K, Kitagawa A and Takada E 1997 *Phys. Rev.* A **55** 808
Trautmann D and Rösel 1980 *Nucl. Instrum. Methods* **169** 259
Tseng H K and Pratt R H 1971 *Phys. Rev.* A **3** 100
Tseng H K, Pratt R H and Lee C M 1977 *Phys. Rev.* A **19** 187
Yamadera A, Ishii K, Sera K, Sebata M and Morita S 1981 *Phys. Rev.* A **23** 24